European Journal of Medicinal Chemistry 63 (2013) 85–94

Contents lists available at SciVerse ScienceDirect

European Journal of Medicinal Chemistry

journal homepage: http://www.elsevier.com/locate/ejmech

Original article

Synthesis and structure–activity relationship studies in serotonin 5-HT_{1A} receptor agonists based on fused pyrrolidone scaffolds

Andrea Cappelli [a,*], Monica Manini [a], Salvatore Valenti [a], Federica Castriconi [a], Germano Giuliani [a], Maurizio Anzini [a], Simone Brogi [a], Stefania Butini [a], Sandra Gemma [a], Giuseppe Campiani [a], Gianluca Giorgi [b], Laura Mennuni [c], Marco Lanza [c], Antonio Giordani [c], Gianfranco Caselli [c], Ornella Letari [c], Francesco Makovec [c]

[a] Dipartimento Farmaco Chimico Tecnologico and European Research Centre for Drug Discovery and Development, Università degli Studi di Siena, Via A. Moro, 53100 Siena, Italy

[b] Dipartimento di Chimica, Università degli Studi di Siena, Via A. Moro, 53100 Siena, Italy

[c] Rottapharm Madaus, Via Valosa di Sopra 9, 20052 Monza, Italy

ARTICLE INFO

Article history:
Received 12 November 2012
Received in revised form
14 January 2013
Accepted 17 January 2013
Available online 8 February 2013

Keywords:
Serotonin
5-HT1A receptors
Arylpiperazine
Binding

ABSTRACT

A new class of serotonin 5-HT_{1A} receptor ligands related to NAN-190, buspirone and aripiprazole has been designed using our potent 5-HT_3 receptor ligands as templates. The designed pyrrolidone derivatives **10a–n** were prepared by means of the straightforward chemistry consisting in the reaction of the appropriate γ-haloester derivatives with the suitable arylpiperazinylalkylamines. The nanomolar 5-HT_{1A} receptor affinity and the agonist-like profile shown by fused pyrrolidone derivatives **10k,m** stimulated the rationalization of the interaction with an homology model of the 5-HT_{1A} receptor and the evaluation of their selectivity profiles and the pharmacokinetic properties. Interestingly, the results of the profiling assays suggested for close congeners **10k,m** a significantly divergent binding pattern with compound **10m** showing an appreciable selectivity for 5-HT_{1A}R.

1. Introduction

Serotonin (5-hydroxytryptamine, 5-HT) is an important neurotransmitter both in central nervous system and in periphery. 5-HT has to date been shown to bind to distinct receptors subdivided into 14 separate subtypes (5-HT_{1-7}: 5-HT_{1A-F}, 5-HT_{2A-C}, 5-HT_3, 5-HT_4, 5-HT_{5A}, 5-HT_6, 5-HT_7) [1]. The 5-HT_{1A} receptor (5-HT_{1A}R) subtype pharmacology has been extensively studied by means of a huge series of developed selective ligands as pharmacological tools (e.g. 8-OH-DPAT, **1** and NAN-190, **2** Fig. 1). Although **2** was earlier considered a selective 5-HT_{1A}R antagonist, evidence was later collected about its alpha2-adrenergic receptor antagonist properties [2]. 5-HT_{1A}R agonists and partial agonists are clinically used in the treatment of anxiety and depression [3]. Buspirone (**3**, Fig. 1) is an example of a psychoactive drug used in the treatment of generalized anxiety disorder of very mild to moderate intensity without panic attacks. Compound **3** was reported to behave as 5-HT_{1A}R partial agonist endowed with moderate 5-HT_{1A}R selectivity (due to its affinity toward other monoaminergic receptors such as dopamine D_2 and adrenergic alpha1 and alpha2 receptor subtypes) [4]. Accordingly, the selectivity issue represents a crucial feature in the development of buspirone-related analogs. Clinically, the interaction with 5-HT_{1A}R is also responsible for the lack of undesired side-effects in some atypical antipsychotic drugs [5]. The serotoninergic system plays a pivotal role in regulation of prefrontal cortex (PFC) functions, including emotional control, cognitive behavior and working memory. PFC pyramidal neurons and GABA interneurons contain a high density of 5-HT_{1A}R and 5-HT_{2A}R. It was demonstrated in PFC that NMDA receptors channels are the target of 5-HT_{1A}R and both receptors modulate the excitability of cortical

Abbreviations: 5-HT, 5-hydroxytryptamine; GPCRs, G-protein coupled receptors; 5-HT_{1A}R, 5-HT_{1A} receptor; PFC, prefrontal cortex; GABA, gamma aminobutyric acid; NMDA, N-methyl-D-aspartate; 5-HT_{2A}R, 5-HT_{2A} receptor; EPS, extrapyramidal symptoms; 5-HT_3R, 5-HT_3 receptor; FPC, fused pyrrolidone component; APC, arylpiperazine component; AC, aryl component; CNS, central nervous system; CA, Central Activity; CR, central reactivity; NR, neurovegetative reflexes; NT, neuromotor tonus; AS, autonomic system; DMEM, Dulbecco's modified eagle medium; IBMX, 3-isobutyl-1-methylxanthine; OPLS-AA, optimized potentials for liquid simulations-all atom; PRCG, Polak-Ribierè conjugate gradient; GB/SA, generalized-born/surface-area.

* Corresponding author. Tel.: +39 0577 234320; fax: +39 0577 234333.
E-mail addresses: andrea.cappelli@unisi.it, cappelli@unisi.it (A. Cappelli).

0223-5234/$ – see front matter
http://dx.doi.org/10.1016/j.ejmech.2013.01.044

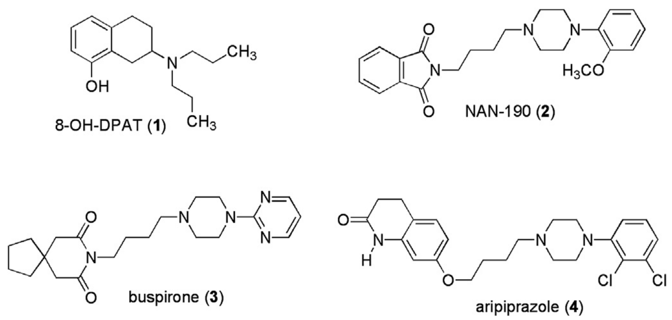

Fig. 1. Structures of some relevant serotonin 5-HT_{1A}R ligands.

neurons thus affecting cognitive functions [6]. Indeed, a variety of preclinical data has suggested that the 5-HT_{1A}R may be a therapeutic target for the development of improved antipsychotics. Although the role of 5-HT_{1A}R in antipsychotic drug efficacy profile is still under debate, 5-HT_{1A}R affinity contributes to the clinical efficacy of most of the atypical antipsychotics (e.g. clozapine, olanzapine, aripiprazole, **4** Fig. 1) and contributes to their low EPS liability [7]. Experimental evidences show that 5-HT_{1A}R activation attenuates antipsychotic-induced side effects in humans [8]. Accordingly, an association was postulated between agonist activity at 5-HT_{1A}R and anxiolytic or antidepressant effects, improvements in cognitive and negative symptoms [9], and decreased development of EPS in schizophrenia [10]. Furthermore, i*n vivo* studies demonstrated that activation of 5-HT_{1A}R can play a role in aripiprazole-mediated behavior in rats [11,12]. Moreover, since glutamatergic transmission is dysfunctional in schizophrenia and glutamate release is decreased by 5-HT_{1A}R activation [13], agonist properties at postsynaptic 5-HT_{1A}R may be relevant to the therapeutic profile of atypical antipsychotic agents, improving negative symptoms and cognitive deficits [14].

Our earlier interest in the search of new serotoninergic agents led to development of a series of chemically diverse compounds endowed with different affinity profiles, selectivity and pharmacological properties [15]. Among the multitude of developed 5-HT receptors ligands, derivatives **5**–**8** (Fig. 2) based on the pyrrolidone structure [16], proved to behave as potent 5-HT_3R ligands. These analogs showed different functional profiles ranging from the antagonist properties of tropane derivatives (compounds **5**–**8** with Het = *endo*-tropan-3-yl) to the full range of intrinsic efficacies shown by the quinuclidine derivatives (compounds **5**–**8** with Het = quinuclidin-3-yl). On the whole, the results obtained suggested that the basic heterocyclic (*endo*-tropan-3-yl or quinuclidin-3-yl) moiety of compounds **5**-**8** governs the long range interaction with the 5-HT_3R and the fused pyrrolidone scaffold plays a significant role in the modulation of the short range contacts. On the other hand, in the series of 3,4-dihydropyrazino[1,2-*a*]indol-1(2*H*)-one-2-yl series of analogs (exemplified by **9a,b**) the 5-HT_{1A}R affinity appeared to be modulated by the functionalization at the arylpiperazine moiety [15c,d].

Taken together, these analyses, prompted us to further explore 5-HT_{1A}R pharmacology. Thus, in the progress of our large program focused on the medicinal chemistry of 5-HT receptor ligands, pyrrolidone derivatives **5**–**8**, NAN-190 (**2**), and compounds **9a**,**b** were considered as structural templates in the design of new 5-HT_{1A}R ligands **10** (Fig. 2), in which the basic heterocyclic moiety employed was the arylpiperazine scaffold widely embodied in most of the known serotoninergic ligands (e.g. **2** and **4**). As the arylpiperazine scaffold is known to interact with a broad range of different receptors, our working hypothesis was the possible modulation of the selectivity by means of the appropriate variation and combination of three structural components, namely: the fused pyrrolidone component (FPC), the spacer between piperazine and pyrrolidone, and the substituents of the arylpiperazine component (APC).

The present paper describes the synthesis and the preliminary pharmacological characterization of 5-HT_{1A}R ligands **10** as well as the pharmacokinetic properties and the rationalization of the ligand–receptor interaction of the most interesting compounds of the series.

2. Results and discussion

2.1. Chemistry

Target pyrrolidone derivatives **10a**–**n** were prepared by means of the simple general procedure (Scheme 1) previously developed for the synthesis of our tropane 5-HT_3R antagonists **5**–**8** [16]. The reaction of appropriate γ-haloester derivative (**11**–**13**) [16] with the suitable arylpiperazinylalkylamine (**14**–**18**) [17] afforded the expected tricyclic ligand (**10a**–**n**) in acceptable to good yields.

The structure of compound **10c** was confirmed by crystallographic studies (Fig. 3) and used as an input in the molecular modeling studies.

2.2. Binding assays, structure–activity relationships (SARs), and molecular modeling studies

The newly developed arylpiperazines **10a**–**n** were evaluated for their potential activity in inhibiting the specific binding of [^{3}H]8-OH-DPAT [18] (**1**) to 5-HT_{1A}R in rat hippocampus membranes in comparison with unlabeled **1**, and the results of the binding studies are summarized in Table 1.

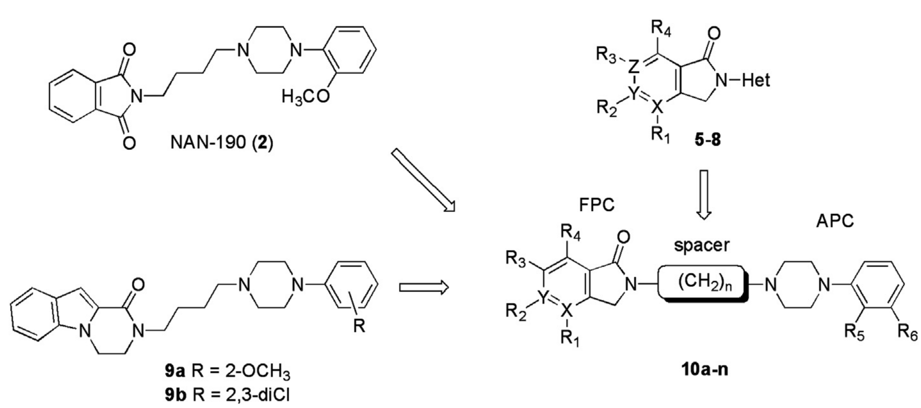

Fig. 2. Design of 5-HT_{1A}R ligands **10a**–**n**. For the specific structure of compounds **10a**–**n** see Table 1.

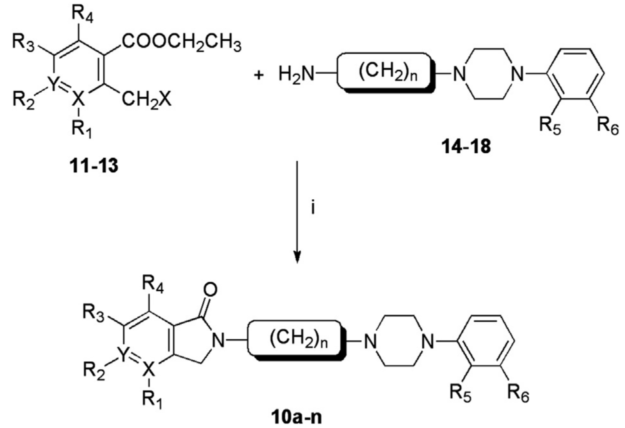

Scheme 1. Synthesis of target compounds **10a**–**n**. For the specific structure of compounds **10a**–**n** see Table 1. Reagents: (i) C_2H_5OH.

In order to better understand the ligand-5-HT_{1A}R interactions for the compounds herein reported, and aiming at investigating the binding mode of these new inhibitors, in the absence of a 3D X-ray structure of the 5-HT_{1A} GPCR, a docking procedure (performed with AutoDock [19]) was applied by using a specific homology model of the 5-HT_{1A}R generated by means of a multiple templates-based homology modeling approach (see experimental section for details) [20]. We chose to make use of multiple templates in the modeling the 5-HT_{1A}R for increasing the quality of the obtained model [21,22]. Indeed, this method successfully allowed us to increase the simulation time for minimizing and optimizing the 5-HT_{1A}R model. The 5-HT_{1A}R affinities shown by compounds **10a**–**n** were found to vary from the submicromolar to the nanomolar range with a modulation appropriate for structure affinity relationship analysis. The most outstanding results were obtained with compounds **10k**,**m**, which are very potent ligands showing *K*i values in the low nanomolar range. In these two arylpiperazine ligands, the combination of the angularly fused pyrrolidone components with the pentamethylene spacer and the 2-methoxyphenyl arylpiperazine component represents the optimal scaffold for the interaction with the 5-HT_{1A}R binding site, which appears to be practically unable to distinguish between compound **10k** ($Ki = 1.6$ nM) and its closely related analog **10m** ($Ki = 1.7$ nM). Interestingly, our computational studies revealed that **10k** and **10m** share virtually identical interactions within 5-HT_{1A}R binding site (Fig. 4).

Particularly, both compounds can establish a T-shaped interaction with the hydrophobic Phe166, and H-bonds with both Asn217 and Arg244. An additional charge-assisted H-bond can take place between the protonated piperazine nitrogen and the carboxylic moiety of Asp78. This pattern of interaction is in line with the nanomolar potency of these 5-HT_{1A}R ligands. The proposed binding modes are also consistent with the experimentally

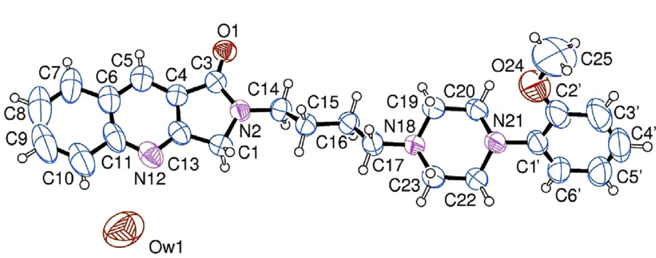

Fig. 3. Structure of compound **10c** found by crystallography. Ellipsoids enclose 50% probability.

Table 1
5-HT_{1A}R binding affinities of compounds **10a**–**n**.

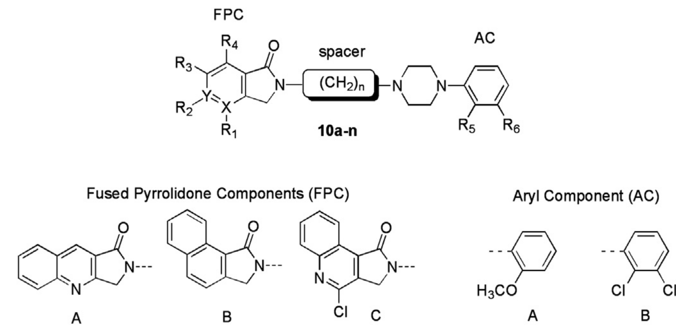

Compd	FPC	Spacer	AC	*K*i (nM) ± SEM[a]
10a	A	$-(CH_2)_3-$	A	104 ± 50
10b	B	$-(CH_2)_3-$	A	46 ± 21
10c	A	$-(CH_2)_4-$	A	15 ± 6
10d	A	$-(CH_2)_4-$	B	30 ± 9
10e	B	$-(CH_2)_4-$	A	13 ± 1
10f	B	$-(CH_2)_4-$	B	31 ± 11
10g	C	$-(CH_2)_4-$	A	17 ± 5
10h	C	$-(CH_2)_4-$	B	31 ± 10
10i	A	$-(CH_2)_5-$	A	20 ± 6
10j	A	$-(CH_2)_5-$	B	58 ± 19
10k	B	$-(CH_2)_5-$	A	1.6 ± 0.2
10l	B	$-(CH_2)_5-$	B	490 ± 125
10m	C	$-(CH_2)_5-$	A	1.7 ± 0.3
10n	C	$-(CH_2)_5-$	B	878 ± 228
1	–	–	–	1.2 ± 0.2

[a] Each value is the mean ± SEM of 3 independent determinations performed in duplicate and represents the concentration giving half the maximum inhibition of [^{3}H]**1** (final concentration 0.5 nM) specific binding to rat cerebral hippocampus membranes.

determined lower activity of compounds **10i** and **10j** (Table 1), since, when compared with **10k** and **10m**, they only revealed the H-bond with the Asn217 (Fig. 5).

The alteration of the optimized combination of the above-mentioned structural components (namely: the angularly fused pyrrolidone components, the pentamethylene spacer, and the 2-methoxyphenyl arylpiperazine component) produces a significant decrease in the 5-HT_{1A}R binding affinity. For instance, the replacement of the 2-methoxyphenyl arylpiperazine component of the best ligands **10k**,**m**, with the 2,3-dichlorophenyl counterpart (as in compounds **10l**,**n**) leads to a dramatic decrease in the 5-HT_{1A}R binding affinity (**10l** vs **10k** and **10n** vs **10m**). Docking studies performed with our arylpiperazine derivatives **10i**,**k**,**m**, highlight that the methoxy group of these compounds is accommodated into a small binding pocket, which appears to be less tolerant for the two chlorine atoms of **10j** (Fig. 6).

On the other hand, the same 2-methoxyphenyl to 2,3-dichlorophenyl replacement appears to be well tolerated in the remaining couples of arylpiperazine ligands reported in Table 1. The very similar affinity shown by **10b**–**j** suggests that apart from the above cited optimized combination of the structural components, a broad range of different combinations is recognized by the receptor with very similar binding energies producing *K*i values about one order of magnitude higher than those shown by the most potent compounds **10k**,**m**. From another point of view, the 5-HT_{1A}R binding site appears to be barely discriminating for compounds bearing the tetramethylene spacer, while it becomes more sensitive when the spacer is homologated to the pentamethylene one. However, when the pentamethylene spacer is combined with the linearly-fused pyrrolidone moiety as in compounds **10i**,**j**, the 2-methoxyphenyl to 2,3-dichlorophenyl replacement appears to be well tolerated as already observed in the tetramethylene

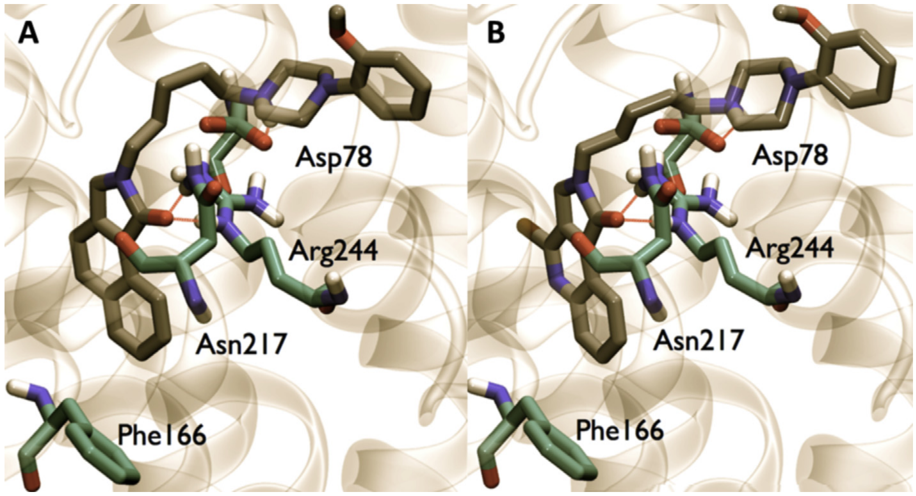

Fig. 4. Interactions of **10k** (panel A) and **10m** (panel B) with the 5-HT$_{1A}$R homology model: Only the relevant aminoacidic residues of the binding site are displayed. Compounds **10k** and **10m** are represented as sticks. The H-bonds are represented as dashed red lines. For sake of clarity only polar hydrogens of the interacting residues and for protonation of piperazine N are displayed. (For interpretation of the references to color in this figure legend, the reader is referred to the web version of this article.)

derivatives **10c**–**h** (compare **10i** vs **10j**). The superimposition of the computational binding complexes of **10k** and **10j** with the receptor depicted in Fig. 6 clearly evidences the perfect fitting of the pyrrolidone component and of the 2-methoxyphenyl arylpiperazine component of **10k** within the two binding cavities of the receptor.

It is noteworthy that the structure–affinity relationship analysis in the pentamethylene derivatives reveals a discrepancy between the 2-methoxyphenyl and the 2,3-dichloromethyl subseries. In fact, the angularly fused derivatives **10k**,**m** belonging to the 2-methoxyphenyl subseries are about one order of magnitude more potent than the corresponding linearly fused **10i**, while angularly fused derivatives **10l**,**n** belonging to the 2,3-dichlorophenyl subseries are about one order of magnitude less potent than the corresponding linearly fused **10j**.

Finally, in compounds **10a**,**b** based on a trimethylene spacer the replacement of the angularly-fused pyrrolidone component of **10b** with the linearly-fused counterpart of **10a** leads to a negligible (two-fold) increase in the 5-HT$_{1A}$R binding affinity.

The most potent compounds binding 5-HT$_{1A}$R in rat hippocampus membranes (i. e. **10k**,**m**) were assayed at Cerep (Poitiers, France) for their potential interaction with 79 off-target receptors (see Supplementary material) in order to evaluate the level of the selectivity reached by these novel arylpiperazine derivatives. The selected ligands were tested firstly at high concentration (e.g. 10,000 nM) and the receptors interacting at significant extents with the ligands were considered for further studies at lower concentrations (e.g. 100 and 10 nM) and affinity estimation for those compounds showing significant inhibitions in the low nanomolar range (Table 2). The profiling assays showed a significantly divergent binding pathway for **10k**,**m**. Very interestingly, 5-HT$_{1A}$R ligand **10m** revealed an appreciable selectivity for the receptor of interest since it was found to interact with only two off-target receptors with affinity values in the low nanomolar range (the estimated affinity values shown for D$_3$, 5-HT$_{2B}$ resulted about one order of magnitude lower than that shown for 5-HT$_{1A}$R). On the other hand, compound **10k** was found to interact also with dopamine D$_{2S}$

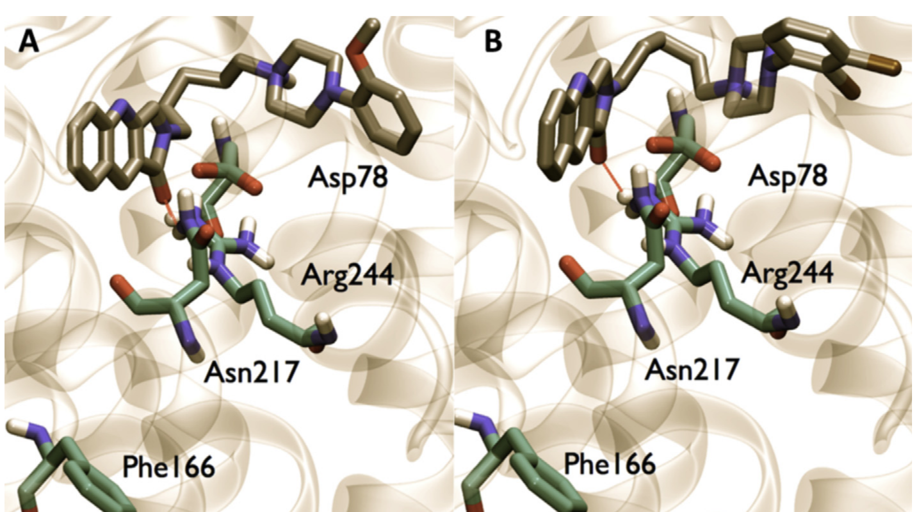

Fig. 5. Interactions of compounds **10i** (panel A) and **10j** (panel B) with the 5-HT$_{1A}$R homology model: Only the relevant aminoacidic residues of the binding site are displayed. Compounds **10i** and **10j** are represented as sticks. The H-bonds are represented as dashed red lines. For sake of clarity only polar hydrogens of the interacting residues and for protonation of piperazine N are displayed. (For interpretation of the references to color in this figure legend, the reader is referred to the web version of this article.)

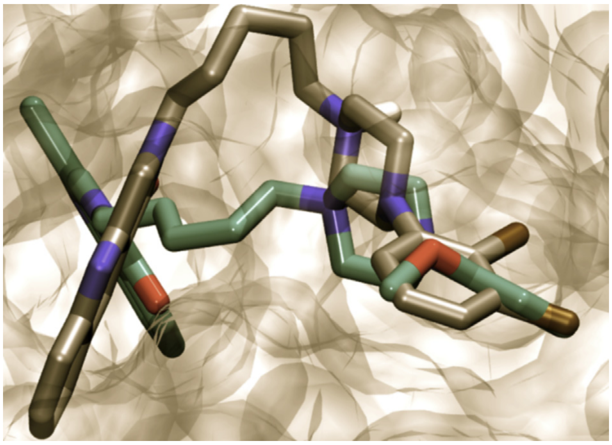

Fig. 6. Superimposition of the computational complexes of ligands **10k** and **10j** with the 5-HT$_{1A}$R homology model binding site. Ligands are represented as licorice colored green and brown for **10k** and **10j** respectively. Protein is represented as transparent brown surface. (For interpretation of the references to color in this figure legend, the reader is referred to the web version of this article.)

receptors (e.g. at 100 and 10 nM, **10k** produced inhibition values very similar to those observed with 5-HT$_{1A}$R) and, to a lesser extent, with D$_3$, D$_4$, 5-HT$_{2B}$, and 5-HT$_7$. Based on these *in vitro* binding data, compound **10k** can rather be considered a "dirty drug" being endowed with an *in vitro* profile highly resembling that of aripiprazole [10]. It should be stressed that the divergent binding profile showed by close congeners **10k**,**m** is accompanied by about the same affinity for 5-HT$_{1A}$R. This observation suggests that in GPCR family the selectivity of ligand–receptor interaction is affected by very minor structural alterations.

2.3. *In vitro 5-HT$_{1A}$R cellular functional assay*

Based on their interesting 5-HT$_{1A}$R binding affinities, compounds **10k**,**m** were selected for a suitable functional characterization in a cellular model. Thus, the agonist-like properties of **10k**,**m** at human 5-HT$_{1A}$ receptors expressed in transfected cell lines were determined *in vitro* by measuring a single signal transduction representing inhibition of adenylyl cyclase activity (cAMP) [23]. Both **10k**,**m** showed agonist-like properties by inhibiting forskolin-stimulated cAMP accumulation: 100 nM **10k**,**m** inhibited by 63% and 60% the adenylyl cyclase signals, respectively. Conversely, **10k**,**m** were unable to reverse the cAMP response evoked by 8-OH-DPAT showing no antagonist-like effect in this cellular system.

2.4. *In vivo pharmacokinetic study*

Because of their potent interaction with 5-HT$_{1A}$R and the promising agonist-like properties, the pharmacokinetic profile of **10k**,**m** was evaluated in mice by using standard protocols and the results are summarized in Table 3. Both compounds are characterized by a very high volume of distribution, being approx 20 and 80 times the theoretical total body water in mice, respectively, and by a high clearance, being their Cl values approx 2 and 4-fold the normal hepatic blood flow in mice [24]. Nevertheless, their absolute oral bioavailability was found to be moderate for **10k** (20%) and relatively high for **10m** (45%), suggesting a relatively good absorption from the gastrointestinal tract.

Table 2
Interaction of compounds **10k**,**m** with off-target receptors.

	10k Inhibition[a] at 100 nM	**10k** Inhibition[a] at 10 nM	**10k** IC$_{50}$ (nM)	**10m** Inhibition[a] at 100 nM	**10m** Inhibition[a] at 10 nM	**10m** IC$_{50}$ (nM)
5-HT$_{2B}$	70	28	43	65	18	63
5-HT$_7$	65	18	62	42	24	>100
D$_{2S}$	90	74	3.5	26	NT	>100
D$_3$	86	39	24	74	38	31
D$_4$	60	13	65	28	10	>100

[a] The inhibition studies were performed at Cerep (Poitiers, France)

2.5. *In vivo safety assays*

Compounds **10k**,**m** were evaluated in the Irwin test [25] in order to obtain preliminary data about the safety of compounds. In summary, male CD1 mice ($n = 3$/group) were dosed with **10k**,**m** up to 80 mg/kg, and kept under observation for the suitable time after drug administration. Analysis of the results showed that neither **10k** nor **10m** affected the behavioral and physiological state of mice as assessed by evaluating 43 different parameters categorized into 5 fundamental activities: Central Activity (CA), Central Reactivity (CR), Neurovegetative Reflexes (NR), Neuromotor Tonus (NT), and Autonomic System (AS).

3. Conclusion

A new series of 5-HT$_{1A}$R ligands was designed using our pyrrolidone 5-HT$_3$R ligands **5**–**8**, compounds **9a**,**b**, NAN-190, buspirone, and aripiprazole as templates. Target derivatives **10a**–**n** were prepared by means of the straightforward chemistry (previously developed for the synthesis of our tropane 5-HT$_3$R antagonists **5**–**8**) based on the reaction of the appropriate γ-haloester derivatives with the proper arylpiperazinylalkylamines. Among the newly-synthesized compounds, **10k**,**m** revealed 5-HT$_{1A}$R affinity values in the low nanomolar range that were easily rationalized in terms of interaction with an homology model of the 5-HT$_{1A}$R. Moreover, profiling assays revealed for the close congeners **10k**,**m** a significantly divergent binding pattern. In particular, compound **10m** showed an appreciable selectivity for 5-HT$_{1A}$R, while **10k** appeared to be a "dirty drug" showing an *in vitro* profile, which resembles that of aripiprazole. In cellular functional studies, fused pyrrolidone derivatives **10k**,**m** showed clear-cut agonist-like profiles. The combination of these results with both the safety profile emerged from the Irwin test results and the reasonable pharmacokinetic profiles suggested that the biological features of arylpiperazine derivatives could be tailored by means of an appropriate chemical design in order to obtain dirty drugs or cleaner agents following the specific needs.

4. Experimental

4.1. *Chemistry*

4.1.1. *General procedures*

All chemicals used were of reagent grade. Yields refer to purified products and are not optimized. Melting points were determined in open capillaries on a Gallenkamp apparatus and are uncorrected. Merck silica gel 60 (230–400 mesh) was used for column chromatography. Merck TLC plates, silica gel 60 F$_{254}$ were used for TLC. ^{1}H NMR spectra were recorded by means of a Bruker AC 200, a Varian Mercury-300, or a Bruker DRX 400 AVANCE spectrometers in the indicated solvents (TMS as internal standard); the values of the chemical shifts are expressed in ppm and the coupling constants (J) in Hz. Mass spectra were recorded on either a Thermo-Finnigan LCQ-Deca or an Agilent 1100 LC/MSD. The purity of compounds **10a**–**n** was assessed by RP-HPLC and was found to be higher than 95%. An Agilent 1100 Series system equipped with a

Table 3
Pharmacokinetic parameters of compounds **10k**,**m** in mice.

Compd	Route	Dose (mg/kg)	Cl (mL/h/kg)	Vz (mL/kg)	t1/2 (h)	AUC 0-t (h*ng/mL)	AUC inf (h*ng/mL)	F%	Cmax (ng/mL)	Tmax (h)
10k	IV	2	9540	17552	1.3	207	210	–	–	–
10k	PO	10	–	–	4.7	212	325	20	56	0.3
10m	IV	2	26400	58708	1.5	70	76	–	–	–
10m	PO	10	–	–	4.5	157	239	45	35	1.0

Lichrocart 125-4 (4 × 125 mm, Purospher Star RP-18C, 5 μm) column was used in the HPLC analysis with acetonitrile-water-methanol (80:10:10) as the mobile phase at a flow rate of 0.5 mL/min. UV detection was achieved at 254 nm.

*4.1.2. General procedure for the synthesis of compounds **10a**–**n***

A mixture of the appropriate γ-haloester derivative (**11**–**13**, 1.0 equivalent) in ethanol with the suitable arylpiperazinylalkylamine (**14**–**18**, 2.0 equivalents) was heated under reflux for the appropriate time (the reaction was monitored by TLC). The reaction mixture was concentrated under reduced pressure and the residue was partitioned between dichloromethane and water. The organic layer was dried over sodium sulfate and concentrated under reduced pressure. Purification of the residue by flash-chromatography with the appropriate eluent gave the corresponding target arylpiperazine derivative (**10a**–**n**).

*4.1.3. 2-[3-[4-(2-Methoxyphenyl)piperazin-1-yl]propyl]-2,3-dihydro-1H-pyrrolo[3,4-b]quinolin-1-one (**10a**)*

This compound was prepared from γ-chloroester **11** [16] (0.10 g, 0.40 mmol) and 3-[4-(2-methoxyphenyl)piperazin-1-yl]propan-1-amine [17a] (**14**, 0.20 g, 0.80 mmol, reaction time = 9 h) and purified by flash-chromatography with ethyl acetate-triethylamine (9:1) as the eluent to obtain pure **10a** as a white solid (0.13 g, yield 78%). An analytical sample was obtained by recrystallization from *n*-hexane-dichloromethane (mp 118–119 °C). ^{1}H NMR (400 MHz, $CDCl_3$): 1.98 (m, 2H), 2.52 (t, *J* = 7.3, 2H), 2.65 (m, 4H), 3.05 (m, 4H), 3.78 (t, *J* = 7.1, 2H), 3.83 (s, 3H), 4.61 (s, 2H), 6.82–6.98 (m, 4H), 7.61 (m, 1H), 7.81 (m, 1H), 7.99 (d, *J* = 8.2, 1H), 8.13 (d, *J* = 8.4, 1H), 8.60 (s, 1H). MS (ESI): *m*/*z* 417 (M + H^+).

*4.1.4. 2-[3-[4-(2-Methoxyphenyl)piperazin-1-yl]propyl]-2,3-dihydro-1H-benzo[e]isoindol-1-one (**10b**)*

This compound was synthesized from γ-bromoester **12** [16] (0.13 g, 0.44 mmol) and amine **14** [17a] (0.22 g, 0.89 mmol, reaction time = 6 h) and purified by flash-chromatography with ethyl acetate-triethylamine (9:1) as the eluent to obtain pure **10b** as a pale yellow glassy solid (0.12 g, yield 65%). ^{1}H NMR (200 MHz, $CDCl_3$): 1.97 (m, 2H), 2.52 (t, *J* = 7.3, 2H), 2.66 (m, 4H), 3.11 (m, 4H), 3.74 (t, *J* = 7.0, 2H), 3.83 (s, 3H), 4.46 (s, 2H), 6.81–6.99 (m 4H), 7.50–7.68 (m, 3H), 7.88–7.98 (m, 2H), 9.25 (d, *J* = 8.1, 1H). MS (ESI): *m*/*z* 416 (M + H^+).

*4.1.5. 2-[4-[4-(2-Methoxyphenyl)piperazin-1-yl]butyl]-2,3-dihydro-1H-pyrrolo[3,4-b]quinolin-1-one (**10c**)*

This compound was synthesized from γ-chloroester **11** [16] (0.12 g, 0.48 mmol) and 4-[4-(2-methoxyphenyl)piperazin-1-yl]butan-1-amine [17a] (**15**, 0.32 g, 1.2 mmol, reaction time = 18 h) and purified by flash-chromatography with ethyl acetate-triethylamine (9:1) as the eluent to obtain pure **10c** as a white solid (0.16 g, yield 77%). An analytical sample was obtained by recrystallization from *n*-hexane-dichloromethane (mp 124–125 °C). ^{1}H NMR (200 MHz, $CDCl_3$): 1.51–1.83 (m, 4H), 2.43 (t, *J* = 7.2, 2H), 2.59 (m, 4H), 3.03 (m, 4H), 3.71 (t, *J* = 7.0, 2H), 3.80 (s, 3H), 4.53 (s, 2H), 6.78–6.97 (m, 4H), 7.56 (t, *J* = 7.3, 1H), 7.77 (t, *J* = 7.3, 1H), 7.94 (d, *J* = 8.0, 1H). 8.09 (d, *J* = 8.5, 1H), 8.55 (s, 1H). MS (ESI): *m*/*z* 431 (M + H^+).

*4.1.6. 2-[4-[4-(2,3-Dichlorophenyl)piperazin-1-yl]butyl]-2,3-dihydro-1H-pyrrolo[3,4-b]quinolin-1-one (**10d**)*

This compound was synthesized from γ-chloroester **11** [16] (0.10 g, 0.40 mmol) and 4-[4-(2,3-dichlorophenyl)piperazin-1-yl]butan-1-amine [17b] (**16**, 0.24 g, 0.80 mmol, reaction time = 6 h) and purified by flash-chromatography with ethyl acetate-triethylamine (8:2) as the eluent to obtain pure **10d** as a white solid (0.13 g, yield 70%). An analytical sample was obtained by recrystallization from *n*-hexane-dichloromethane (mp 154–155 °C). ^{1}H NMR (400 MHz, $CDCl_3$): 1.58–1.85 (m, 4H), 2.48 (t, *J* = 7.3, 2H), 2.62 (m, 4H), 3.04 (m, 4H), 3.76 (t, *J* = 7.1, 2H), 4.59 (s, 2H), 6.93 (m, 1H), 7.12 (m, 2H), 7.62 (t, *J* = 7.4, 1H), 7.83 (t, *J* = 7.0, 1H), 8.07 (d, *J* = 8.2, 1H), 8.14 (d, *J* = 8.4, 1H), 8.60 (s, 1H). MS (ESI): *m*/*z* 469 (M + H^+).

*4.1.7. 2-[4-[4-(2-Methoxyphenyl)piperazin-1-yl]butyl]-2,3-dihydro-1H-benzo[e]isoindol-1-one (**10e**)*

This compound was synthesized from γ-bromoester **12** [16] (0.18 g, 0.61 mmol) and amine **15** [17a] (0.32 g, 1.2 mmol, reaction time = 5 h) and purified by flash-chromatography with ethyl acetate-triethylamine (9:1) as the eluent to obtain pure **10e** as a pale yellow oil, which crystallized on standing (0.14 g, yield 53%). An analytical sample was obtained by recrystallization from *n*-hexane-dichloromethane (mp 128–129 °C). ^{1}H NMR (400 MHz, $CDCl_3$): 1.60–1.79 (m, 4H), 2.48 (t, *J* = 7.2, 2H), 2.65 (m, 4H), 3.08 (m, 4H), 3.75 (t, *J* = 7.0, 2H), 3.84 (s, 3H), 4.42 (s, 2H), 6.82–6.98 (m, 4H), 7.45–7.65 (m, 3H), 7.91–7.95 (m, 2H), 9.25 (d, *J* = 8.2, 1H). MS (ESI): *m*/*z* 430 (M + H^+).

*4.1.8. 2-[4-[4-(2,3-Dichlorophenyl)piperazin-1-yl]butyl]-2,3-dihydro-1H-benzo[e]isoindol-1-one (**10f**)*

This compound was synthesized from γ-bromoester **12** [16] (0.18 g, 0.61 mmol) and amine **16** [17b] (0.37 g, 1.2 mmol, reaction time = 6 h) and purified by flash-chromatography with ethyl acetate-triethylamine (8:2) as the eluent to obtain pure **10f** as a pale yellow oil, which crystallized on standing (0.075 g, yield 26%, mp 92–93 °C). ^{1}H NMR (200 MHz, $CDCl_3$): 1.58–1.82 (m, 4H), 2.47 (t, *J* = 7.4, 2H), 2.62 (m, 4H), 3.04 (m, 4H), 3.72 (t, *J* = 7.1, 2H), 4.45 (s, 2H), 6.93 (m, 1H), 7.12 (m, 2H), 7.48-7.68 (m, 3H), 7.90 (d, *J* = 8.1, 1H), 7.98 (d, *J* = 8.4, 1H). 9.23 (d, *J* = 9.0, 1H). MS (ESI): *m*/*z* 468 (M + H^+).

*4.1.9. 4-Chloro-2-[4-[4-(2-methoxyphenyl)piperazin-1-yl]butyl]-2,3-dihydro-1H-pyrrolo[3,4-c]quinolin-1-one (**10g**)*

This compound was prepared from γ-bromoester **13** [16] (0.41 g, 1.25 mmol) with amine **15** [17a] (0.66 g, 2.5 mmol, reaction time = 6 h) and purified by flash-chromatography with ethyl acetate-triethylamine (9:1) as the eluent to give compound **10g** as a pale yellow oil, which crystallized on standing (0.27 g, yield 46%, mp 126–127 °C). ^{1}H NMR (200 MHz, $CDCl_3$): 1.57–1.86 (m, 4H), 2.46 (t, *J* = 7.2, 2H), 2.63 (m, 4H), 3.06 (m, 4H), 3.72 (t, *J* = 6.9, 2H), 3.81 (s, 3H), 4.47 (s, 2H), 6.80–6.99 (m, 4H), 7.63–7.81 (m, 2H), 8.06 (d, *J* = 8.1, 1H), 8.98 (d, *J* = 7.9, 1H). MS (ESI): *m*/*z* 465 (M + H^+).

4.1.10. 4-Chloro-2-[4-[4-(2,3-dichlorophenyl)piperazin-1-yl]butyl]-2,3-dihydro-1H-pyrrolo[3,4-c]quinolin-1-one (**10h**)

This compound was prepared from γ-bromoester **13** [16] (0.41 g, 1.25 mmol) with amine **16** [17b] (0.75 g, 2.5 mmol, reaction time = 6 h) and purified by flash-chromatography with ethyl acetate as the eluent to obtain compound **10h** as a white solid (0.28 g, yield 45%). An analytical sample was obtained by recrystallization from *n*-hexane-dichloromethane (mp 140–141 °C). ^{1}H NMR (200 MHz, $CDCl_3$): 1.55–1.88 (m, 4H), 2.47 (t, $J = 7.2$, 2H), 2.62 (m, 4H), 3.05 (m, 4H), 3.76 (t, $J = 7.0$, 2H), 4.52 (s, 2H), 6.92 (m, 1H), 7.13 (m, 2H), 7.66–7.85 (m, 2H), 8.11 (d, $J = 8.4$, 1H), 9.03 (d, $J = 8.5$, 1H). MS (ESI): m/z 503 (M + H$^+$).

4.1.11. 2-[5-[4-(2-Methoxyphenyl)piperazin-1-yl]pentyl]-2,3-dihydro-1H-pyrrolo[3,4-b]quinolin-1-one (**10i**)

This compound was synthesized from γ-chloroester **11** [16] (0.10 g, 0.40 mmol) and 5-[4-(2-methoxyphenyl)piperazin-1-yl]pentan-1-amine [17c] (**17**, 0.22 g, 0.80 mmol, reaction time = 21 h) and purified by flash-chromatography with ethyl acetate-triethylamine (9:1) as the eluent to obtain pure **10i** as a pale yellow oil (0.14 g, yield 79%). An analytical sample was obtained by recrystallization from *n*-hexane-dichloromethane (mp 116–118 °C). ^{1}H NMR (200 MHz, $CDCl_3$): 1.34–1.78 (m, 6H), 2.38 (t, $J = 7.4$, 2H), 2.58 (m, 4H), 3.04 (m, 4H), 3.69 (t, $J = 7.1$, 2H), 3.81 (s, 3H), 4.53 (s, 2H), 6.78-6.98 (m, 4H), 7.57 (t, $J = 7.3$, 1H), 7.78 (t, $J = 7.1$, 1H), 7.95 (d, $J = 8.6$, 1H), 8.10 (d, $J = 8.5$, 1H), 8.56 (s, 1H). MS (ESI): m/z 445 (M + H$^+$).

4.1.12. 2-[5-[4-(2,3-Dichlorophenyl)piperazin-1-yl]pentyl]-2,3-dihydro-1H-pyrrolo[3,4-b]quinolin-1-one (**10j**)

This compound was synthesized from γ-chloroester **11** [16] (0.10 g, 0.40 mmol) and 5-[4-(2,3-dichlorophenyl)piperazin-1-yl]pentan-1-amine [17b] (**18**, 0.25 g, 0.79 mmol, reaction time = 24 h) and purified by flash-chromatography with ethyl acetate-triethylamine (8:2) as the eluent to obtain pure **10j** as a pale yellow oil, which crystallized on standing (0.13 g, yield 67%). An analytical sample was obtained by recrystallization from *n*-hexane-dichloromethane (mp 93–95 °C). ^{1}H NMR (200 MHz, $CDCl_3$): 1.38–1.84 (m, 6H), 2.40 (t, $J = 7.3$, 2H), 2.59 (m, 4H), 3.02 (m, 4H), 3.72 (t, $J = 7.1$, 2H), 4.56 (s, 2H), 6.90 (m, 1H), 7.11 (m, 2H), 7.60 (t, $J = 7.6$, 1H), 7.81 (t, $J = 7.8$, 1H), 7.98 (d, $J = 7.8$, 1H), 8.12 (d, $J = 8.5$, 1H), 8.59 (s, 1H). MS (ESI): m/z 483 (M + H$^+$).

4.1.13. 2-[5-[4-(2-Methoxyphenyl)piperazin-1-yl]pentyl]-2,3-dihydro-1H-benzo[e]isoindol-1-one (**10k**)

This compound was synthesized from γ-bromoester **12** [16] (4.1 g, 14 mmol) and amine **17** [17c] (7.8 g, 28 mmol, reaction time = 6 h) and purified by flash-chromatography with ethyl acetate-triethylamine (9:1) as the eluent to obtain pure **10k** as a pale yellow glassy solid (2.6 g, yield 42%). ^{1}H NMR (200 MHz, $CDCl_3$): 1.34–1.81 (m, 6H), 2.40 (t, $J = 7.4$, 2H), 2.62 (m, 4H), 3.05 (m, 4H), 3.67 (t, $J = 7.1$, 2H), 3.83 (s, 3H), 4.41 (s, 2H), 6.80–7.01 (m, 4H), 7.44–7.67 (m, 3H), 7.86–7.97 (m, 2H), 9.24 (d, $J = 8.2$, 1H). MS (ESI): m/z 444 (M + H$^+$5.

4.1.14. 2-[5-[4-(2,3-Dichlorophenyl)piperazin-1-yl]pentyl]-2,3-dihydro-1H-benzo[e]isoindol-1-one (**10l**)

This compound was prepared from γ-bromoester **12** [16] (0.12 g, 0.41 mmol) and amine **18** [17b] (0.26 g, 0.82 mmol, reaction time = 12 h) and purified by flash-chromatography with ethyl acetate-triethylamine (9:1) as the eluent to obtain pure **10l** as a pale yellow oil, which crystallized on standing (0.080 g, yield 40%, mp 90–91 °C). ^{1}H NMR (200 MHz, $CDCl_3$): 1.42–1.82 (m, 6H), 2.41 (t, $J = 7.3$, 2H), 2.60 (m, 4H), 3.02 (m, 4H), 3.70 (t, $J = 7.2$, 2H), 4.43 (s, 2H), 6.88 (m, 1H), 7.09 (m, 2H), 7.46–7.67 (m, 3H), 7.87–7.98 (m, 2H), 9.24 (d, $J = 8.3$, 1H). MS (ESI): m/z 482 (M + H$^+$).

4.1.15. 4-Chloro-2-[5-[4-(2-methoxyphenyl)piperazin-1-yl]pentyl]-2,3-dihydro-1H-pyrrolo[3,4-c]quinolin-1-one (**10m**)

This compound was synthesized from γ-bromoester **13** [16] (12 g, 36.5 mmol) and amine **17** [17c] (20 g, 72 mmol, reaction time = 6 h) and purified by flash-chromatography with ethyl acetate-triethylamine (9:1) as the eluent to obtain pure **10m** as a pale glassy solid (2.5 g, yield 14%). ^{1}H NMR (200 MHz, $CDCl_3$): 1.35–1.85 (m, 6H), 2.42 (t, $J = 7.3$, 2H), 2.64 (m, 4H), 3.07 (m, 4H), 3.70 (t, $J = 7.2$, 2H), 3.83 (s, 3H), 4.47 (s, 2H), 6.80–7.00 (m, 4H), 7.63-7.82 (m, 2H), 8.07 (d, $J = 8.5$, 1H), 9.01 (d, $J = 8.1$, 1H). MS (ESI): m/z 479 (M + H$^+$).

4.1.16. 4-Chloro-2-[5-[4-(2,3-dichlorophenyl)piperazin-1-yl]pentyl]-2,3-dihydro-1H-pyrrolo[3,4-c]quinolin-1-one (**10n**)

This compound was prepared from γ-bromoester **13** [16] (0.10 g, 0.30 mmol) and amine **18** [17b] (0.19 g, 0.61 mmol, reaction time = 5 h) and purified by flash-chromatography with ethyl acetate-triethylamine (9:1) as the eluent to obtain pure **10n** as a white solid (0.092 g, yield 59%). An analytical sample was obtained by recrystallization from ethyl acetate-dichloromethane (mp 181–182 °C). ^{1}H NMR (200 MHz, $CDCl_3$): 1.43–1.86 (m, 6H), 2.42 (t, $J = 7.3$, 2H), 2.61 (m, 4H), 3.03 (m, 4H), 3.73 (t, $J = 7.2$, 2H), 4.50 (s, 2H), 6.90 (m, 1H), 7.12 (m, 2H), 7.66-7.84 (m, 2H), 8.11 (d, $J = 8.6$, 1H), 9.05 (d, $J = 8.0$, 1H). MS (ESI): m/z 517 (M + H$^+$).

4.2. X-ray crystallography

Single crystals of compound **10c** were submitted to X-ray data collection on a Siemens P4 diffractometer with a graphite monochromated Mo-Kα radiation ($\lambda = 0.71073$ Å) at 293 K. The structure was solved by direct methods implemented in SHELXS-97 program [26]. The refinement was carried out by full-matrix anisotropic least-squares on F^2 for all reflections for non-H atoms by means of the SHELXL-97 program [27]. Crystallographic data (excluding structure factors) for the structure solved in this paper have been deposited with the Cambridge Crystallographic Data Centre as supplementary publication CCDC 877453. Copies of the data can be obtained, free of charge, on application to CCDC, 12 Union Road, Cambridge CB2 1EZ, UK; (fax: + 44 (0) 1223 336 033; or e-mail: deposit@ccdc.cam.ac.uk).

4.3. In vitro pharmacological studies

4.3.1. Binding assays

Male Wistar rats (Charles River Italia, Calco, CO, Italy) weighing 200–250 g were used. Animal care and handling throughout the experimental procedures were in accordance with the European Communities Council Directive of 24 November 1986 (86/609/EEC).

Rats were sacrificed by decapitation, brains were rapidly dissected and hippocampi were used for binding assay preparation according to Hall et al. [18] Crude membranes were diluted in the binding buffer (Tris-Cl 50 mM, pH 7.4) in order to obtain the final protein concentration.

[^{3}H]8-OH-DPAT specific binding was measured in 0.5 mL total volume. Aliquots (50 μL) of tissue suspension (3 mg/mL protein concentration) were incubated with 50 μL of 0.5 nM labeled ligand (Perkin Elmer Life and Analytical Sciences), and different concentrations of the compound under investigation. Five to eight concentrations of each compound were assayed, each performed in duplicate. The incubation was performed in polypropylene test tubes at 37 °C for 10 min. The bound radioligand was separated by rapid filtration on glass fiber Whatman GF/C filters. Filtrates were washed four times with 4 mL of cold binding buffer, before the filter disks were transferred in minivials filled with 4 mL of Ultima Gold (Perkin Elmer Life and Analytical Sciences).

The specific binding of [^{3}H]8-OH-DPAT (final concentration 0.5 nM) was defined as the difference between the total binding and the nonspecific binding determined in the presence of 10 μM 5-HT and represented about 80–85% of the total binding.

Competition experiments were analyzed by the “Allfit” program [28] to obtain the concentration of unlabeled drug that caused 50% inhibition of [^{3}H]8-OH-DPAT specific binding (IC_{50}). Apparent affinity constants (K_i) were derived from the IC_{50} values according to the Cheng and Prusoff equation [$K_i = IC_{50}/(1 + L/K_d)$] [29].

The binding of compounds **10k**,**m** to human recombinant D_{2S} receptors expressed in HEK-293 cells was assayed following described methods [30]. The specific binding of [^{3}H] spiperone (final concentration 0.3 nM; incubation 22 °C for 1 h) was determined as the difference between the total binding and the nonspecific binding determined in the presence of 1.0 μM unlabeled (+)-butaclamol.

4.3.2. 5-HT_{1A}R cellular functional assays

Cyclic AMP accumulation was determined in CHO cells transfected with the human 5-HT_{1A}R receptor as previously described [31]. Briefly, cells were incubated (22 °C for 15 min) with compounds **10k** or **10m** in DMEM, 10 mM HEPES, 100 mM forskolin, and 100 mM 3-isobutyl-1-methylxanthine (IBMX). The reaction was stopped by aspiration of the medium and addition of 0.1 N HCl. Data were expressed as % of the response obtained with 100 nM 8-OH-DPAT (agonist effect) and/or as % of inhibition of control 10 nM 8-OH-DPAT stimulus (antagonist effect).

4.4. In vivo pharmacokinetic studies

Male CD1 mice (20–30 g; Charles River Labs, France) were fasted overnight prior to dosing. Two groups of mice ($n = 3$) were dosed intravenously (iv) at 2 mg/kg with both **10k**,**m**. Sampling time points were 5, 15, 30, 60, 120, 240, 360, and 1440 min after iv administration of each tested compound. Two additional groups of mice ($n = 3$) were dosed orally at 10 mg/kg. Sampling time points were 15, 30, 60, 120, 240, 360, 480 and 1440 min after oral administration of each tested compound. Blood was drawn by a cardiac puncture at each time point and collected in tubes coated with lithium heparin, mixed gently, then kept on ice and centrifuged at 2500 g for 15 min at 4 °C, within 1 h of collection. Plasma was then harvested and stored at −20 °C prior to analysis.

4.5. In vivo safety assay (Irwin test)

General behavioral observations were recorded by camera. Male CD1 mice ($n = 3$/group; Harlan, S.Pietro al Natisone, UD, Italy) were dosed orally with **10k**,**m** up to 80 mg/kg. Compounds were suspended in a solution containing 0.1% Tween 80 + 0.5% methyl cellulose (Sigma–Aldrich, Milan) and administered in a volume of 10 mL/kg. Animals were kept under observation for a total time of 24 h after a single oral administration of drugs.

4.6. Molecular modeling

4.6.1. Homology modeling

The sequence of rat 5-HT_{1A}R was taken in fasta format from the UniProtKB (entry P19327) [32]. The template selection was performed by HOMER-A (HOmology ModellER) using automatic template search method (version 1.3) [33]. In the automatic template selection mode the web-server application searched for a template structure for the modeling of the target sequence using the PDB-BLAST protocol [34]. This procedure was performed in two steps: in the first step, the target sequence was used as a seed to construct an exhaustive sequence profile on the non-redundant protein sequence database. In the second step, the previously obtained profile was used to scan the PDB database of known protein structure for possible templates. Usage of the exhaustive profile drastically increases the probability to find a suitable template structure [35]. Following this approach three best templates with higher sequence identity were selected in order to build the 3D structure of the 5-HT_{1A}R. The sequences of *h*β2-adrenergic receptor (Protein Data Bank code 2RH1; sequence identity of chain A 36.9%), *t*β1-adrenergic receptor (2VT4; sequence identity of chain B 29.7%) and *h*$A2_A$ adenosine receptor (3EML; sequence identity of chain A 22.7%) were imported into Prime [36] and aligned to the query sequence. Subsequently, these templates 3D structures aligned were used for “Comparative Modeling” methods implemented in Prime. Since we aligned multiple templates, which in Prime can be used in several ways to build a model, we specified, in the “build structure step”, which method was used for building the 5-HT_{1A}R 3D structure. Consensus model option was employed to build the model; this option allowed us to take into account all the previously selected templates since the model was built as an average of all templates. The obtained model was submitted to refinement protocol in Prime environment. In particular, we have performed a side-chains optimization and loops refinement by Prime and default settings were employed. Further structure optimization was carried out by MacroModel application implemented in Maestro [37] suite 2011 using the Optimized Potentials for Liquid Simulations-all atom (OPLS-AA) force field 2005 [38]. The solvent effects were simulated using the analytical Generalized-Born/Surface-Area (GB/SA) model [39], and no cutoff for non-bonded interactions was selected. Polak-Ribierè Conjugate Gradient (PRCG) method with 100,000 maximum iterations and 0.001 gradient convergence threshold was employed. Moreover, the minimized 5-HT_{1A}R homology model was submitted to Protein Preparation Wizard Workflow implemented in Maestro suite 2011 [40]. This protocol allowed us to obtain a reasonable starting structure of the receptor for our molecular docking calculations, by a series of computational steps. In particular, we performed three steps in order to: i) add missed hydrogens; ii) optimize the orientation of hydroxyl groups, Asn, and Gln, and the protonation state of His; and iii) perform a constrained refinement with the impref utility, setting the max root-mean-square deviation (RMSD) of 0.30 Å. The impref utility consists of a cycles of energy minimizations based on the impact molecular mechanics engine and on the OPLS_2005 force field.

The modeled protein was validated by Ramachandran plot (see Supplementary material) generated by RAMPAGE webserver [41]. The residues of protein were for 82.4% (336 amino acids) in the favored region of the plot, 17.2% (70 amino acids not involved in the binding site) of the residues lie in additional allowed region and only 0.5% (2 amino acids not involved in the binding site) of the residues were located in the disallowed region as depicted in. The results of RAMPAGE webserver revealed that over 99% of the residues of our 5-HT_{1A}R refined model sit in the allowed regions of Ramachandran Plot. This value is more than the cut-off value (96.1%) defined for the most reliable models [42]. Consequently, the stereo chemical quality of our 5-HT_{1A}R homology model was found acceptable displaying a very low percentage of residues having phi/psi angles in outlier region.

4.6.2. Ligand setup

Starting from our experimental X-ray data the structures of the ligands used in the docking simulations were generated by means of Macmolplt [43], and were optimized by means of GAMESS [44]. Ligand Optimizations and partial atomic point charges calculations were performed with RHF and 6-31g* as basis set. All the relevant torsion angles were treated as rotatable during the docking process, thus allowing a search of the conformational space.

4.6.3. Receptor setup

The homology model of 5-HT_{1A}R was setup for docking as follows: receptor was prepared by protein preparation wizard protocol implemented in Maestro as described in the homology modeling section, and Kollman united-atom partial charges were as-signed. The ADDSOL utility of AutoDock was used to add solvation parameters to the protein structures, and the grid maps representing the proteins in the docking process were calculated using AutoGrid. The grids, one for each atom type in the inhibitor plus one for the electrostatic interactions, were chosen to be large enough to include not only the hypothetical channel binding site sites but also a significant part of the protein around it. As a consequence, the dimensions of the grid maps were 100 × 100 × 100 points, with a grid-point spacing of 0.375 Å.

4.6.4. Docking calculations

All the docked compounds were subjected to 256 independent runs of docking simulations by means of the AutoDock 4.2 [19] using the Lamarckian genetic algorithm and through a protocol with an initial population of 300 randomly placed individuals, a maximum number of 50 million energy evaluations, a mutation rate of 0.02, a crossover rate of 0.80, and an elitism value of 1. The pseudo-Solis and Wets algorithm with a maximum of 300 interactions was applied for the local search. 256 independent docking runs were carried out for each ligand, and the resulting conformations that differed by less than 2.0 Å in positional RMSD were clustered together. Cluster analysis was performed by selecting the lowest energy solution of the most populated cluster. The lowest energy solutions resulting from the docking calculations in each case belong to the most populated cluster; the most populated clusters were taken into account for their consistency with experimental data. All estimated binding energies was in agreement with the nanomolar range of the biological data. All protonated conformations were optimized and the point charges were obtained by means of *ab-initio* calculations, and then used into the docking simulations.

Acknowledgments

The authors are grateful to Dr. Francesco Berrettini (CIADS, Università di Siena) for the X-ray data collection. This work was partly supported by MIUR (Ministero dell'Istruzione, dell'Università e della Ricerca) - PRIN (Programmi di ricerca di Rilevante Interesse Nazionale).

Appendix A. Supplementary data

Supplementary data related to this article can be found at http://dx.doi.org/10.1016/j.ejmech.2013.01.044.

References

[1] J. Hannon, D. Hoyer, Molecular biology of 5-HT receptors, Behav. Brain Res. 195 (2008) 198–213.
[2] J.P. Foong, J.C. Bornstein, 5-HT antagonists NAN-190 and SB 269970 block alpha2-adrenoceptors in the guinea pig, Neuroreport 20 (2009) 325–330.
[3] R. Schreiber, J. De Vry, 5-HT1A receptor ligands in animal models of anxiety, impulsivity and depression: multiple mechanisms of action? Prog. Neuro-Psychopharmacol. Biol. Psychiatry 17 (1993) 87–104.
[4] G. Tunnicliff, Molecular basis of buspirone's anxiolytic action, Pharmacol. Toxicol. 69 (1991) 149–156.
[5] A.C. McCreary, C.A. Jones, Antipsychotic medication: the potential role of 5-HT(1A) receptor agonism, Curr. Pharm. Des. 16 (2010) 516–521.
[6] P. Zhong, E.Y. Yuen, Z. Yan, Modulation of neuronal excitability by serotonin-NMDA interactions in prefrontal cortex, Mol. Cell. Neurosci. 38 (2008) 290–299.
[7] (a) S.L. Mason, G.P. Reynolds, Clozapine has sub-micromolar affinity for 5-HT_{1A} receptors in human brain tissue, Eur. J. Pharmacol. 221 (1992) 397–398;
(b) J. Elliott, G.P. Reynolds, Agonist-stimulated GTPgamma[^{35}S] binding to 5-HT1A receptors in human post-mortem brain, Eur. J. Pharmacol. 386 (1999) 313–315;
(c) E. Richelson, T. Souder, Binding of antipsychotic drugs to human brain receptors. Focus on newer generation compounds, Life Sci. 68 (2000) 29–39.
[8] K. Yoshida, T. Sugita, H. Higuchi, Y. Hishikawa, Effect of tandospirone on tardive dyskinesia and parkinsonian symptoms, Eur. Psychiatry 13 (1998) 421–422.
[9] M.J. Millan, Improving the treatment of schizophrenia: focus on serotonin 5-HT_{1A} receptors, J. Pharmacol. Exp. Ther. 295 (2000) 853–861.
[10] D.A. Shapiro, S. Renock, E. Arrington, L.A. Chiodo, L.X. Liu, D.R. Sibley, B.L. Roth, R. Mailman, Aripiprazole, a novel atypical antipsychotic drug with a unique and robust pharmacology, Neuropsychopharmacology 28 (2003) 1400–1411.
[11] D. Marona-Lewicka, D.E. Nichols, Aripiprazole (OPC-14597) fully substitutes for the 5-HT_{1A} receptor agonist LY293284 in the drug discrimination assay in rats, Psychopharmacology 172 (2004) 415–421.
[12] S. Jordan, V. Koprivica, R. Chen, K. Tottori, T. Kikuchi, C.A. Altar, The antipsychotic aripiprazole is a potent, partial agonist at the human 5-HT_{1A} receptor, Eur. J. Pharmacol. 441 (2002) 137–140.
[13] F. Mauler, T. Fahrig, E. Horvath, R. Jork, Inhibition of evoked glutamate release by the neuroprotective 5-HT_{1A} receptor agonist BAY X 3702 *in vitro* and in vivo, Brain Res. 888 (2001) 150–157.
[14] H.Y. Meltzer, T. Sumiyoshi, Does stimulation of 5-HT_{1A} receptors improve cognition in schizophrenia? Behav. Brain Res. 195 (2008) 98–102.
[15] (a) A. Cappelli, M. Anzini, S. Vomero, L. Mennuni, F. Makovec, M. Hamon, P.G. De Benedetti, M.C. Menziani, The interactions of the 5-HT_3 receptor with arylpiperazine, tropane, and quinuclidine ligands, Curr. Top. Med. Chem. 2 (2002) 599–624;
(b) A. Cappelli, S. Butini, A. Brizzi, S. Gemma, S. Valenti, G. Giuliani, M. Anzini, L. Mennuni, G. Campiani, V. Brizzi, S. Vomero, The interactions of the 5-HT_3 receptor with quipazine-like arylpiperazine ligands: the journey track at the end of the first decade of the third millennium, Curr. Top. Med. Chem. 10 (2010) 504–526;
(c) G. Campiani, S. Butini, F. Trotta, C. Fattorusso, B. Catalanotti, F. Aiello, S. Gemma, V. Nacci, E. Novellino, J.A. Stark, A. Cagnotto, E. Fumagalli, F. Carnovali, L. Cervo, T. Mennini, Synthesis and pharmacological evaluation of potent and highly selective D_3 receptor ligands: inhibition of cocaine-seeking behavior and the role of dopamine D_3/D_2 receptors, J. Med. Chem. 46 (2003) 3822–3839;
(d) S. Butini, S. Gemma, G. Campiani, S. Franceschini, F. Trotta, M. Borriello, N. Ceres, S. Ros, S.S. Coccone, M. Bernetti, M. De Angelis, M. Brindisi, V. Nacci, I. Fiorini, E. Novellino, A. Cagnotto, T. Mennini, K. Sandager-Nielsen, J.T. Andreasen, J. Scheel-Kruger, J.D. Mikkelsen, C. Fattorusso, Discovery of a new class of potential multifunctional atypical antipsychotic agents targeting dopamine D_3 and serotonin 5-HT_{1A} and 5-HT_{2A} receptors: design, synthesis, and effects on behavior, J. Med. Chem. 52 (2009) 151–169.
[16] A. Cappelli, M. Anzini, S. Vomero, L. Mennuni, F. Makovec, E. Doucet, M. Hamon, M.C. Menziani, P.G. De Benedetti, G. Giorgi, C. Ghelardini, S. Collina, Novel potent 5-HT_3 receptor ligands based on the pyrrolidone structure: synthesis, biological evaluation, and computational rationalization of the ligand-receptor interaction modalities, Bioorg. Med. Chem. 10 (2002) 779–801.
[17] (a) A. Hackling, R. Ghosh, S. Perachon, A. Mann, H.D. Holtje, C.G. Wermuth, J.C. Schwartz, W. Sippl, P. Sokoloff, H. Stark, N-(omega-(4-(2-methoxyphenyl) piperazin-1-yl)alkyl)carboxamides as dopamine D_2 and D_3receptor ligands, J. Med. Chem. 46 (2003) 3883–3899;
(b) M.J. Robarge, S.M. Husbands, A. Kieltyka, R. Brodbeck, A. Thurkauf, A.H. Newman, Design and synthesis of [(2,3-dichlorophenyl)piperazin-1-yl] alkylfluorenylcarboxamides as novel ligands selective for the dopamine D_3 receptor subtype, J. Med. Chem. 44 (2001) 3175–3186;
(c) M. Resimont, J.F. Liegeois, Synthesis and *in vitro* binding studies of piperazine-alkyl-naphthamides: impact of homology and sulphonamide/carboxamide bioisosteric replacement on the affinity for 5-HT_{1A}, alpha$_{2A}$, D4.2, D3 and D2L receptors, Bioorg. Med. Chem. Lett. 20 (2010) 5199–5202.
[18] M.D. Hall, S. el Mestikawy, M.B. Emerit, L. Pichat, M. Hamon, H. Gozlan, [^{3}H]8-hydroxy-2-(di-n-propylamino)tetralin binding to pre- and postsynaptic 5-hydroxytryptamine sites in various regions of the rat brain, J. Neurochem. 44 (1985) 1685–1696.
[19] G.M. Morris, D.S. Goodsell, R.S. Halliday, R. Huey, W.E. Hart, R.K. Belew, A.J. Olson, Automated docking using a Lamarckian genetic algorithm and an empirical binding free energy function, J. Comput. Chem. 19 (1998) 1639–1662.
[20] (a) A. Rayan, New vistas in GPCR 3D structure prediction, J. Mol. Model. 16 (2010) 183–191;
(b) M. Li, H. Fang, L. Du, L. Xia, B. Wang, Computational studies of the binding site of alpha$_{1A}$-adrenoceptor antagonists, J. Mol. Model. 14 (2008) 957–966.
[21] (a) J.C. Mobarec, R. Sanchez, M. Filizola, Modern homology modeling of G-protein coupled receptors: which structural template to use? J. Med. Chem. 52 (2009) 5207–5216;
(b) P. Sokkar, S. Mohandass, M. Ramachandran, Multiple templates-based homology modeling enhances structure quality of AT_1 receptor: validation by molecular dynamics and antagonist docking, J. Mol. Model. 17 (2011) 1565–1577.
[22] N. Fernandez-Fuentes, B.K. Rai, C.J. Madrid-Aliste, J.E. Fajardo, A. Fiser, Comparative protein structure modeling by combining multiple templates and optimizing sequence-to-structure alignments, Bioinformatics 23 (2007) 2558–2565.
[23] A. Newman-Tancredi, M.B. Assie, N. Leduc, A.M. Ormiere, N. Danty, C. Cosi, Novel antipsychotics activate recombinant human and native rat serotonin 5-

HT_{1A} receptors: affinity, efficacy and potential implications for treatment of schizophrenia, Int. J. Neuropsychopharmacol. 8 (2005) 341–356.
[24] B. Davies, T. Morris, Physiological parameters in laboratory animals and humans, Pharm. Res. 10 (1993) 1093–1095.
[25] S. Irwin, Comprehensive observational assessment: Ia. A systematic, quantitative procedure for assessing the behavioral and physiologic state of the mouse, Psychopharmacologia 13 (1968) 222–257.
[26] G.M. Sheldrick, SHELXS-97, Rel. 97–2, A Program for Automatic Solution of Crystal Structures, University of Göttingen, Göttingen (Germany), 1997.
[27] G.M. Sheldrick, SHELXL-97, Rel. 97–2, A Program for Crystal Structure Refinement, University of Göttingen, Göttingen (Germany), 1997.
[28] A. DeLean, P.J. Munson, D. Rodbard, Simultaneous analysis of families of sigmoidal curves: application to bioassay, radioligand assay, and physiological dose-response curves, Am. J. Physiol. 235 (1978) E97–E102.
[29] Y. Cheng, W.H. Prusoff, Relationship between the inhibition constant (Ki) and the concentration of inhibitor which causes 50 per cent inhibition (I_{50}) of an enzymatic reaction, Biochem. Pharmacol. 22 (1973) 3099–3108.
[30] D.K. Grandy, M.A. Marchionni, H. Makam, R.E. Stofko, M. Alfano, L. Frothingham, J.B. Fischer, K.J. Burke-Howie, J.R. Bunzow, A.C. Server, et al., Cloning of the cDNA and gene for a human D2 dopamine receptor, Proc. Natl. Acad. Sci. U. S. A. 86 (1989) 9762–9766.
[31] A. Newman-Tancredi, L. Verriele, M.J. Millan, Differential modulation by GTPgammaS of agonist and inverse agonist binding to h5-HT_{1A} receptors revealed by [3H]-WAY100,635, Br. J. Pharmacol. 132 (2001) 518–524.
[32] M. Magrane, the UniProt consortium, UniProt Knowledgebase: A Hub of Integrated Protein Data Database, 2011: Bar009 (2011).
[33] S.C.E. Tosatto, The VICTOR Package for 3D Protein Structure Modelling, http://protein.cribi.unipd.it/homer 2009.
[34] L. Rychlewski, L. Jaroszewski, W. Li, A. Godzik, Comparison of sequence profiles. Strategies for structural predictions using sequence information, Protein Sci. 9 (2000) 232–241.
[35] http://protein.bio.unipd.it/homer/helpauto.html, access date: 10.04.12.
[36] Prime, Version 3.0, Schrödinger, LLC, New York, NY, 2011.
[37] MacroModel, Version 9.9, Schrödinger, LLC, New York, NY, 2011.
[38] (a) W.L. Jorgensen, D.S. Maxwell, J. TiradoRives, Development and testing of the OPLS all-atom force field on conformational energetics and properties of organic liquids, J. Am. Chem. Soc. 118 (1996) 11225–11236;
(b) G.A. Kaminski, R.A. Friesner, J. Tirado-Rives, W.L. Jorgensen, Evaluation and reparametrization of the OPLS-AA force field for proteins via comparison with accurate quantum chemical calculations on peptides, J. Phys. Chem. B 105 (2001) 6474–6487.
[39] W.C. Still, A. Tempczyk, R.C. Hawley, T. Hendrickson, Semianalytical treatment of solvation for molecular mechanics and dynamics, J. Am. Chem. Soc. 112 (1990) 6127–6129.
[40] Protein Preparation Wizard Workflow, http://www.schrodinger.com/supportdocs/18/16., 2011.
[41] S.C. Lovell, I.W. Davis, W.B. Arendall 3rd, P.I. de Bakker, J.M. Word, M.G. Prisant, J.S. Richardson, D.C. Richardson, Structure validation by Calpha geometry: phi, psi and Cbeta deviation, Proteins 50 (2003) 437–450.
[42] R. Luthy, J.U. Bowie, D. Eisenberg, Assessment of protein models with 3-dimensional profiles, Nature 356 (1992) 83–85.
[43] B.M. Bode, M.S. Gordon, MacMolPlt: a graphical user interface for GAMESS, J. Mol. Graph. Model. 16 (1998) 133–138.
[44] K.K. Baldridge, M.S. Gordon, J.H. Jensen, N. Matsunaga, M.W. Schmidt, T.L. Windus, J.A. Boatz, T.R. Cundari, Applications of parallel GAMESS, in: T.G. Mattson (Ed.), Parallel Computing in Computational Chemistry, vol. 592, American Chemical Society, Washington, DC, 1995, pp. 29–46.